Journal of Polymer Research (2024) 31:172
https://doi.org/10.1007/s10965-024-04019-y

ORIGINAL PAPER

Preparation and antibacterial properties of polypropylene composite with bisphenol A-type benzoxazine

Xiaoyu Shang[1] · Changlu Zhou[1] · Xian Zhang[2] · Zhong Xin[1]

Received: 29 January 2024 / Accepted: 22 May 2024 / Published online: 6 June 2024

Abstract

Polypropylene (PP) is a commonly used material in medical supplies. However, its lack of antibacterial properties has led to a frequent occurrence of healthcare-associated infections that need to be addressed. This study extensively investigates the antibacterial effects of bisphenol A-type benzoxazine (BA-a), revealing a relationship between the curing degree of BA-a and its antibacterial performance. A lower degree of curing corresponds to stronger antibacterial activity. At the processing temperature of 170 °C, the curing degree of BA-a reached only 14.6%, and it had strong antibacterial activity. Based on this relationship, a melt blending method at 170 °C is determined to prepare PP/BA-a composite material, aiming to enhance the antibacterial properties. The antibacterial performance of PP/BA-a is evaluated by plate coating method. The results demonstrate that PP/0.8BA-a exhibits an antibacterial rate as high as 99.99% against E. coli and S. aureus. Migration experiments confirm the stability of the antibacterial effect. The extracts from PP/BA-a show no toxicity towards mouse fibroblast cells (L929). Furthermore, compared to pure PP, the addition of BA-a improves the thermal stability of PP/BA-a, with an increase of 56 °C in the onset thermal decomposition temperature ($T_{5\%}$), enabling PP to better adapt to the high-temperature environment of moist heat sterilization. This study presents a novel method for obtaining highly antibacterial medical polymer materials (PP/BA-a) with broad application prospects.

Keywords Polypropylene (PP) · Bisphenol A-type benzoxazine · Antibacterial properties · Melt blending

Introduction

The thermoplastic resin polypropylene (PP) is widely utilized in the medical field due to its exceptional chemical stability and non-cytotoxic properties [1, 2]. However, PP does not have antibacterial properties, which limits its application in the medical field. Biological contamination in clinical environments can result in bacteria attaching to the surface of PP and spreading to new hosts through contact [3, 4], thereby endangering the lives of patients. In the United States alone, hospital-acquired infections (HAIs) are estimated to cause approximately 1.7 million infections and 99,000 related deaths each year [5]. Many bacteria can survive on PP surfaces for over a month [6], posing a6 significant threat to patient health. Therefore, it is crucial to stop this transmission mode, for example, by providing materials that can directly kill bacteria upon contact. Thus, the antibacterial modification of PP holds great significance.

Standard methods for preparing antibacterial polypropylene (PP) include composite preparation, post-processing treatment, and melt blending. The composite preparation method involves the adhesion of antibacterial agents to the surface of PP, typically achieved through injection molding or compression molding. For example, adding nanosilver (Ag) to the zeolitic imidazolate framework-8 (ZIF-8) and then grafting Ag@ZIF-8 onto polypropylene melt-blown nonwoven fabric using a lamination process can achieve an antibacterial rate of 85% [7].

The post-processing treatment method involves impregnating or coating antibacterial agents onto pre-formed plastic products to provide them with surface antibacterial properties. For instance, by using the immersion-pressing-drying-plasma (IPDP) process, quaternary ammonium salt

✉ Zhong Xin
xzh@ecust.edu.cn

[1] Shanghai Key Laboratory of Multiphase Materials Chemical Engineering, East China University of Science and Technology, 130 Meilong Road, Shanghai 200237, People's Republic of China

[2] Department of Urology, Zhongshan Hospital, Fudan University, Shanghai 200032, China

is grafted onto the surface of PP nonwoven fabric to impart good antibacterial and hydrophilic properties [8]. Alternatively, fixing quaternary ammonium salt-modified chitosan (QCS) onto the polymer surface forms an antibacterial coating that enhances the antibacterial effect against Staphylococcus aureus and Pseudomonas aeruginosa by 90% [9]. These methods have the advantages of using a small amount of antibacterial agents and cost-saving. However, they also have the challenges of complex processing and poor antibacterial stability. Once the surface antibacterial layer is peeled off or damaged, the antibacterial effect will be lost.

In order to obtain PP with specific antibacterial stability and easier preparation, melt blending processing method has attracted more and more attention. However, melt blending often requires a high selection of antibacterial agents, which need to have high antibacterial efficiency to ensure low dosage and good compatibility with the PP matrix.

In general, antimicrobial agents suitable for melt blending can be divided into three types: natural antimicrobial agents, inorganic antimicrobial agents, and organic antimicrobial agents. Natural antimicrobial agents are usually derived from animals and plants in nature, such as curcumin [10, 11], chitosan [12], and propolis [13]. This type of antimicrobial agent has advantages such as non-toxicity and strong biocompatibility, but their poor stability, low temperature resistance, and complex processing methods greatly limit their use [14, 15]. Inorganic antimicrobial agents usually refer to metal ions or oxides with antimicrobial activity, including Ag^+ [16–18], TiO_2 [19], ZnO [20] and so on. Inorganic antimicrobial agents have certain advantages in terms of heat resistance, safety, antimicrobial activity, and durability, but they also have some disadvantages such as high cost and poor compatibility. Additionally, inorganic antimicrobial agents are mostly heavy metals, which may cause pollution to the ecological environment, thus causing controversy [21–23].

Organic antibacterial agents have the advantages of significant bactericidal effect, good compatibility, and ease of processing, but they have disadvantages such as high toxicity, poor heat resistance, and poor antibacterial stability [24]. The antibacterial polypropylene composites material (PP-f) containing grafted triclosan (TCS) was prepared through melt blending process [25]. The antibacterial rate of this composite material against Escherichia coli and Staphylococcus aureus exceeds 99%. This indicates that PP-f has excellent antibacterial effects. However, there is still controversy regarding the potential toxicity of TCS to the human body [26, 27]. Therefore, taking potential health risk into consideration, caution should be exercised when using antibacterial materials containing TCS. In order to achieve melt blending as a processing condition and overcome the disadvantages of the above-mentioned antibacterial agents, benzoxazine was chosen as the antibacterial agent. There have been many studies that have used benzoxazine as an antibacterial material and antibacterial drug. Bo et al. synthesized a cardanol-benzoxazine-based thermosetting resin containing bisphenol A dioxane (PCBOz-BD), which achieved inhibition rates of 95% and 99% against E. coli and S. aureus, respectively [28]. Zafar et al. prepared Mg(II)CNSL-FA films, which showed inhibition rates of 12%, 16%, and 50% against E. coli, S. aureus, and Bacillus subtilis, respectively [29]. Mohamed et al. synthesized a bio-based multifunctional benzoxazine (AP-fa-BZ), which exhibited good antibacterial activity [30]. However, most of the current research is focused on the design of benzoxazine-rich molecules and the introduction of different functional groups to enhance their antibacterial properties. Currently, it has been proven that benzoxazine groups have good antibacterial performance [31, 32]. However, there is little research on the antibacterial performance of benzoxazine groups themselves, and there are few reports on blending them into thermoplastic resins.

In this study, Bisphenol A benzoxazine (BA-a) was chosen as the antibacterial agent, and its curing degree and antibacterial activity were investigated through infrared spectroscopy, differential scanning calorimetry (DSC), and antibacterial zone experiments. PP/BA-a antibacterial composites were prepared through melt blending, and its antibacterial performance was evaluated through in vitro antibacterial experiments. The bacterial adhesion on the surface of the material and its morphology were observed using scanning electron microscopy (SEM). The antibacterial stability of PP/BA-a was evaluated through BA-a migration experiments. The cytotoxicity of PP/BA-a towards L929 cells was evaluated through MTT assays. In addition, the crystallization and melting behavior, thermal stability and mechanical properties of PP/BA-a were studied.

Experimental section

Materials and preparation of PP/BA-a composites

In order to further study the curing degree of BA-a in the actual processing process, different temperatures and times were adjusted to explore the effects of processing conditions on the curing degree.

PP was purchased from China Shenhua Energy Company Limited, model K7760H. BA-a was purchased from Keyi polymer Technology Company Limited, model CB3100. Antioxidant was purchased from BASF Corporation

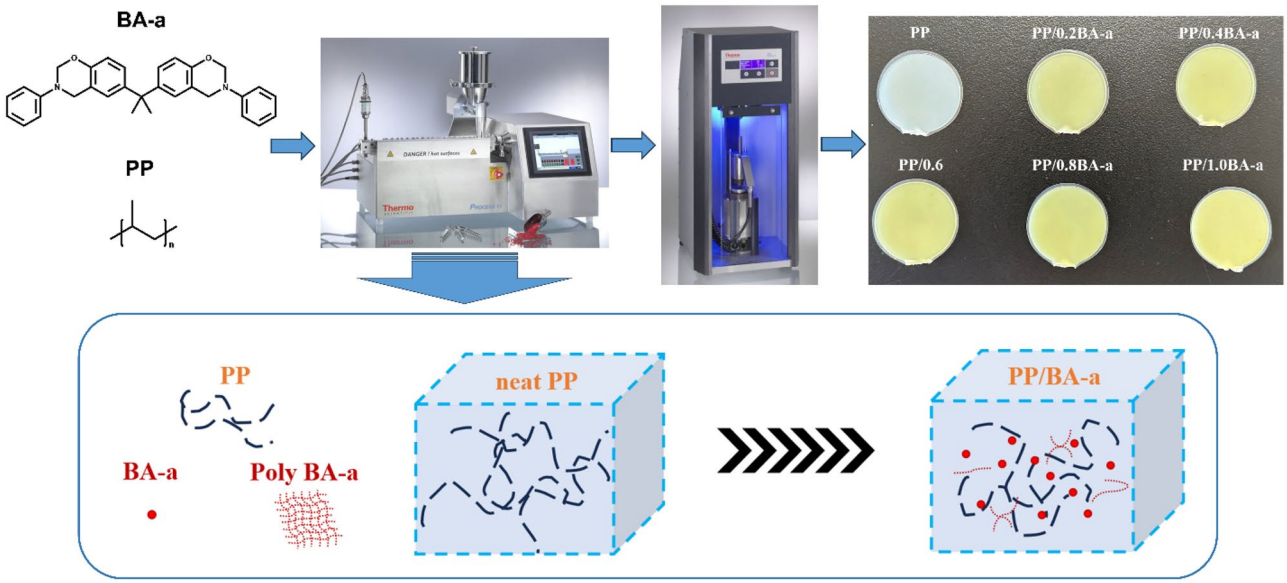

Scheme 1 The preparation of PP/BA-a composites

(Germany), model Irganox 1010 and Irgafos 168. Scheme 1 describes the entire processing process of modified polypropylene PP/BA-a.

Table 1 summarizes the compositions and processing conditions of BA-a and PP/BA-a composites used in this study.

The PP/BA-a were prepared in Mini Extruder (Thermo Fisher, USA) at the mass at 170 °C for 2 min according to the compositions in Table 1. The prepared blends were crushed and made into specimens for mechanical properties tests and antibacterial properties tests with a Haake Minijet Pro (Thermo Fisher, USA). The crushed sample was first melted for 3 min at 170 °C, then injected at 500 bar for 15 s, and finally maintained the pressure of 400 bar for 30 s at 40 °C. The specific preparation method is consistent with the patent [33].

Characterizations of BA-a

Structure of BA-a and Poly BA-a

The structures of BA-a and Poly BA-a were analyzed by Fourier Transform infrared spectroscopy (FTIR) spectrometers (Thermo Fisher, USA). The scanning range is 4000 cm^{-1} to 400 cm^{-1} with a resolution of 4 cm^2. The sample was mixed with spectral grade KBr, and the test sample was obtained by pressing. Each sample was scanned 32 times.

Isothermal curing performance of BA-a

The isothermal curing performance analysis of BA-a was carried out using a differential scanning calorimeter(METTLER, DSC3 + , Switzerland). Weigh 3–5 mg sample and place it

Table 1 Compositions and processing conditions of BA-a and PP/BA-a composites

Sample	PP (g)	BA-a (g)	Irganox 1010 (g)	Irgafos 168 (g)	Temperature (°C)	Time (min)
BA-a	/	5	/	/	/	0
170 °C BA-a	/	5	/	/	170	5
200 °C BA-a	/	5	/	/	200	5
230 °C BA-a	/	5	/	/	230	5
Poly BA-a	/	5	/	/	200	180
PP	100	0	0.1	0.1	170	5
PP/0.2BA-a	100	0.2	0.1	0.1	170	5
PP/0.4BA-a	100	0.4	0.1	0.1	170	5
PP/0.6BA-a	100	0.6	0.1	0.1	170	5
PP/0.8BA-a	100	0.8	0.1	0.1	170	5
PP/1.0BA-a	100	1.0	0.1	0.1	170	5

in an aluminum crucible sample dish. In the environment of nitrogen, the temperature is heated up to 300 °C from 40 °C at the rate of 10 °C /min.

In vitro antibacterial activity

The antibacterial activity of BA-a was explored through the inhibition zone assay. E. coli and S. aureus of 10^6 CFU/mL were prepared, and 100 μL bacterial solution was evenly coated on Luria–Bertani (LB) solid medium. After ultraviolet sterilization, the solid sample is lightly pressed with sterilization tweezers to make it stick to the surface of the medium to ensure full contact between the sample and the medium. The liquid samples were placed on medium with the help of Oxford cups. The medium was cultured in a constant temperature incubator at 37 °C for 24 h. After the culture was completed, the medium was taken out and photographed with the camera, and the size of the antibacterial zone was measured and recorded.

Characterizations of PP/ BA-a composites

In vitro antibacterial activity

PP/BA-a samples were tested for E. coli and S. aureus according to GB/T 31402–2015 test method for antibacterial properties of plastic surface. The bacterial solution with a concentration of 10^5 CFU/mL was prepared, and 100 μL was uniformly dropped on the surface of the sample. Use sterilizing tweezers to gently place the sterilizing film slightly smaller than the sample surface area on the sample. Ensure that the bacterial solution is in uniform contact with the sample, and the bacterial solution does not overflow the sterilization film. The samples were placed in a constant temperature incubator and cultured at 37 °C for 24 h. After that, the bacterial solution on the sample and sterilizing film were eluted, and then the eluent was continuously diluted by a factor of 10 with a sterile Phosphate Buffered Saline (PBS) solution. The dilute solution of 100 μL was evenly coated on LB solid medium and cultured in a constant temperature incubator at 37 °C for 18 h. Count the colonies on the petri dish, control the colonies between 30 and 300, and finally calculate the antibacterial rate based on the number of colonies.

PP and PP/BA-a samples were selected and cultured in suspensions of Escherichia coli and Staphylococcus aureus (1×10^8 CFU/mL) for 24 h. Subsequently, the samples were fixed with a 2.5 wt% aqueous solution of glutaraldehyde at 4 °C for more than 6 h. The surface-unbound bacteria were then washed away with a PBS solution. Afterwards, different concentrations of ethanol (30%, 50%, 70%, 90%, 100%) were used for dehydration treatment, and finally, the bacterial morphology was observed using a scanning electron microscope (SEM).

Antibacterial stability

The antibacterial stability of PP/BA-a was evaluated according to the migration test of BA-a in PP/BA-a. Ultraviolet spectrophotometer (Shimadzu, UV-1750, Japan) was used to determine the UV absorption peaks of benzoxazine with different concentrations in ethyl acetate, ethanol and PBS, and the standard curves were drawn. PP/BA-a samples were immersed in 45 ml ethyl acetate, ethanol and PBS for 1–7 days, respectively. The UV absorption peak value of the leaching solution was measured, and the migration was calculated according to the standard curve.

Cytotoxicity

The cell toxicity of PP/BA-a was tested using the MTT method. Mouse fibroblast cells (L929 cells) were seeded in a 96-well plate at a density of 4×10^3 cells per well, with each well containing 200 μL. The plate was then incubated overnight at a constant temperature of 37 °C in a CO_2 incubator with 5% CO_2. According to ISO 10993–12 2007 standard, the extraction of PP/BA-a was prepared, resulting in a 100% extraction sample. The sample was added to the wells of the plate, and fresh growth medium was replaced. The cells were further incubated for 1–5 days. After pretreatment, the absorbance at 570 nm was measured using an enzyme immunoassay analyzer.

Crystallization behavior

The crystallization behavior analysis of PP/BA-a was carried out using a differential scanning calorimeter (METTLER, DSC3 + , Switzerland). Weigh 3–5 mg sample and place it in an aluminum crucible sample dish. In the environment of nitrogen, the temperature is heated up to 200 °C at the rate of 50 °C /min to eliminate the heat history for 5 min. Then the temperature is reduced to 50 °C at the rate of 10 °C /min to obtain the crystallization curve. Finally, the temperature was heated to 200 °C at the rate of 10 °C/min, and the secondary melting curve was obtained.

The glass transition temperature of the sample was obtained by DMA analyzer (METTLER, Switzerland). The mechanical loss of the sample from 70 °C to 50 °C were measured at a temperature rise rate of 3 °C/min at a frequency of 1 Hz using a double cantilever bending mode.

Thermal stability

Thermogravimetric analysis (TGA) was conducted using TA Instrument (model Q50, USA) system. PP/BA-a samples

(6–10 mg) were heated from 40 °C to 800 °C under nitrogen atmosphere at 10 °C/min.

Mechanical property

Tensile and flexural properties of the samples were measured using a universal testing machine (CMT4204, Shenzhen SANS, China). Prepare samples of $127 \times 12.7 \times 3.2$ mm^3 and dog-bone-shaped samples with 25 mm mark distance. Experiments are performed according to ASTM D790 and ASTM D638, and the final mechanical properties result is the average of at least five measurements. Impact strengths were measured using the electronic simple beam impact tester (XJJD-5 type, Chengde Jinjian Testing Instruments Co., Ltd.) according to ASTM E23-2018.

Results and discussion

Structure changes of BA-a during curing performance

In order to study the structural changes of BA-a before and after curing, FTIR analysis of BA-a and Poly BA-a was performed. The Fig. 1 shows the FTIR comparison of BA-a and Poly BA-a. It can be seen that compared with BA-a, the characteristic peak of the oxazine ring at 948 cm^{-1} of Poly BA-a basically disappeared, indicating that the ring-opening polymerization (ROP) occurred in the oxazine ring. Due to the ROP of the oxazine ring, more Ar–O-C is converted into Ar–O-H structure. Compared with BA-a, the Ar–O-C asymmetric stretching vibration peak in the oxazine ring at 1232 cm^{-1} of Poly BA-a basically disappeared. The absorption peak of Poly BA-a at 3383 cm^{-1} is enhanced, which is the appearance of the characteristic peak of phenol hydroxyl group [34].

Figure 2(a) shows the DSC curves of BA-a under different processing conditions and Poly BA-a. The endothermic peak on the DSC curve represents the melting process of the benzoxazine monomer, while the exothermic peak indicates the ROP of the benzoxazine monomer. According to the curve, at a heating rate of 10 °C/min, the melting point of BA-a is 63 °C, the start temperature of curing is 228 °C, and the peak curing temperature is 240 °C. It is worth noting that the DSC curve represents the heating process, but in the actual processing of PP/BA-a composites, there is no significant temperature increase trend, instead, it follows a relatively isothermal process. To simulate the actual processing, BA-a was kept at constant temperatures of 170 °C, 200 °C, and 230 °C for 5 min respectively, and then heated from 40 °C to 300 °C at a rate of 10 °C/min. The DSC curve still shows an exothermic peak, while Poly BA-a does not exhibit an exothermic peak. This indicates that BA-a cannot fully cure during the processing. In comparison to the BA-a monomer, the peak temperature of the exothermic peak decreases. This suggests that under the mentioned processing conditions, some ROP occurs in BA-a, resulting in the presence of BA-a monomers and partially ring-opened oligomers simultaneously.

In order to further explore the degree of curing of BA-a during the processing, we conducted FTIR spectroscopic analysis on it. Figure 2(b) shows the FTIR spectra of BA-a under different processing conditions. From the curve, it can be observed that as the processing temperature increases, the

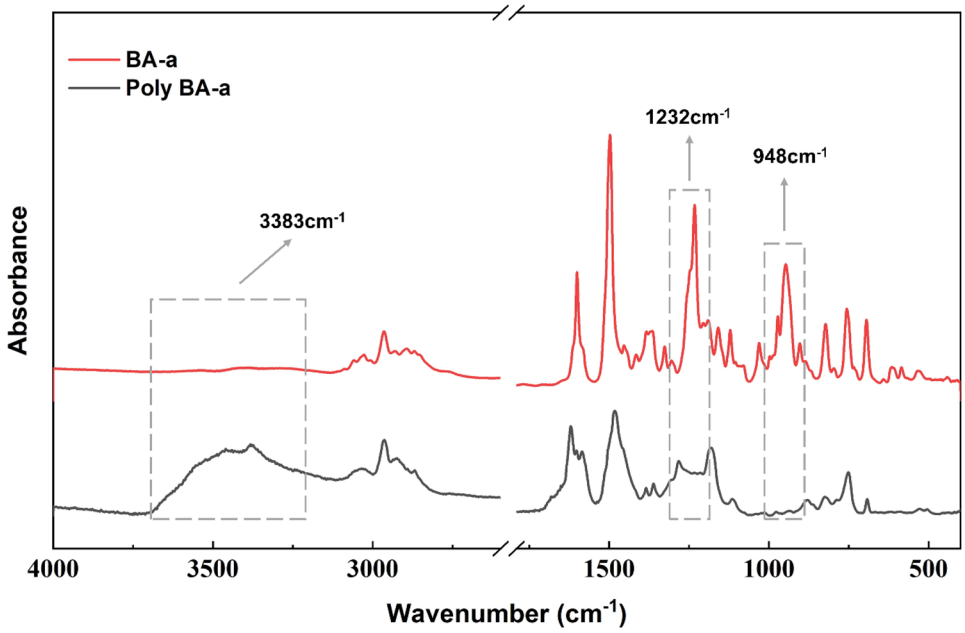

Fig. 1 FTIR spectra before and after BA-a polymerization

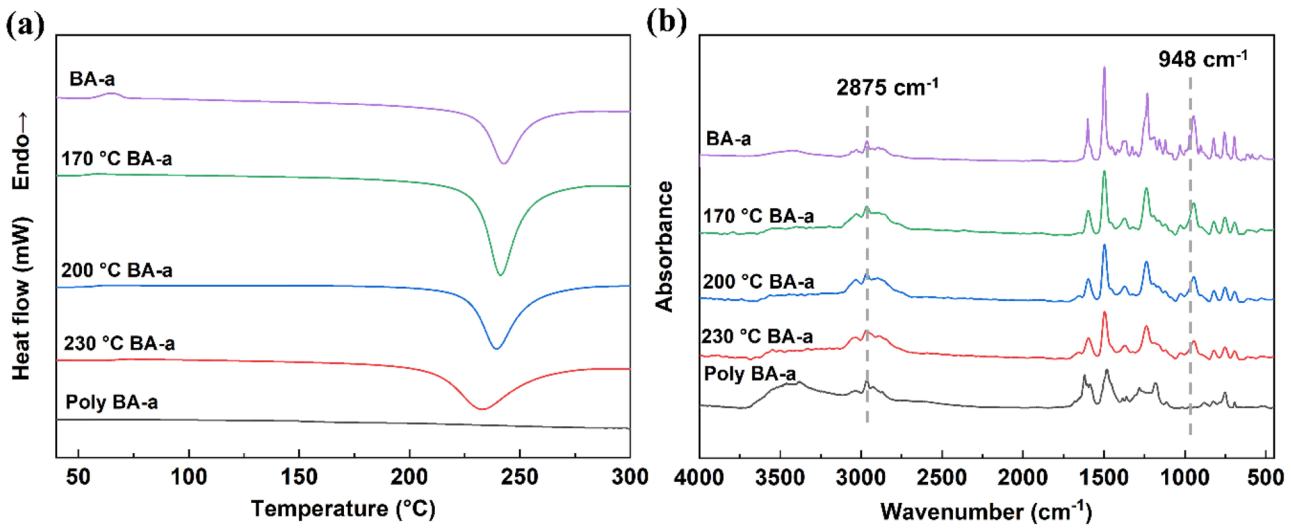

Fig. 2 **a** DSC curves of BA-a under different processing conditions and Poly BA-a; **b** FTIR spectra of BA-a under different processing conditions and Poly BA-a

characteristic peak of the oxazine group at 948 cm^{-1} gradually disappears, indicating an increasing degree of curing of BA-a. To analyze the ring-opening rate of the oxazine group, we calculated the degree of curing of BA-a using the change in peak area of the characteristic peaks in the FTIR spectrum. During the curing process, the -CH_2 antisymmetric stretching peak at 2938 cm^{-1} is considered as an invariant internal reference peak, while the characteristic peak of the oxazine ring at 948 cm^{-1} gradually disappears with the degree of curing [35]. Therefore, the degree of curing of BA-a can be calculated using Eq. (1).

$$\text{Conversion}_{\text{BA-a}} = 1 - \frac{A_{948,X}/A_{2875,X}}{A_{948,BA-a}/A_{2875,BA-a}} \times 100\% \quad (1)$$

By calculation, we can see that the BA-a ring-opening rate processed at different temperatures shows an increasing trend. The specific calculation results are shown in Table 2.

Antibacterial property of BA-a

In this test, Poly BA-a was tested in solid state, while BA-a was tested in solution. BA-a was dissolved in ethyl acetate as the solvent. Additionally, considering that ethyl acetate may have inherent antibacterial properties, ethyl acetate solution was chosen as the blank control. From Fig. 3, it can be observed that BA-a exhibits good antibacterial performance against Escherichia coli and Staphylococcus aureus. However, Poly BA-a has no antibacterial effect, as bacteria continue to grow around the sample without any inhibition zone. Additionally, it can be observed that a higher processing temperature results in a smaller inhibition zone. This indicates that the curing degree of BA-a can influence its antibacterial activity. Further measurements have been made to obtain the specific diameter of inhibition zone, as shown in Table 2.

Table 2 illustrates the degree of curing and the diameter of the antibacterial zone of BA-a. As can be seen from Table 2, BA-a has strong antibacterial activity, but with the increase of curing degree, its antibacterial activity decreases. This is because the antibacterial activity of BA-a is mainly derived from the oxazine ring in its structure. The nitrogen and oxygen lone pairs on the oxazine ring enhance its reducibility, consistent with the biological effectiveness of the oxazine ring[1]. The curing process of BA-a is actually the ROP process of the oxazine ring, resulting in changes in the structure of the oxazine group and the gradual loss of antibacterial activity. The fully open Poly BA-a no longer has the oxazine group, so it has no antibacterial activity. Therefore, the melt blending processing temperature for PP

Table 2 The relationship between curing degree and antibacterial activity

Sample	Degree of curing/%	Diameter of the inhibition zone/mm[a]	
		E. coli	S. aureus
BA-a	0	10.7 ± 0.5	6.4 ± 0.7
170 °C BA-a	14.6	6.6 ± 1.2	3.8 ± 0.4
200 °C BA-a	32.3	3.4 ± 0.6	1.7 ± 0.2
230 °C BA-a	42.6	3.3 ± 0.6	0.8 ± 0.5
Poly BA-a	100	0.0 ± 0.0	0.0 ± 0.0

[a]The diameter here represents the data obtained by subtracting the diameter of the ethyl acetate control

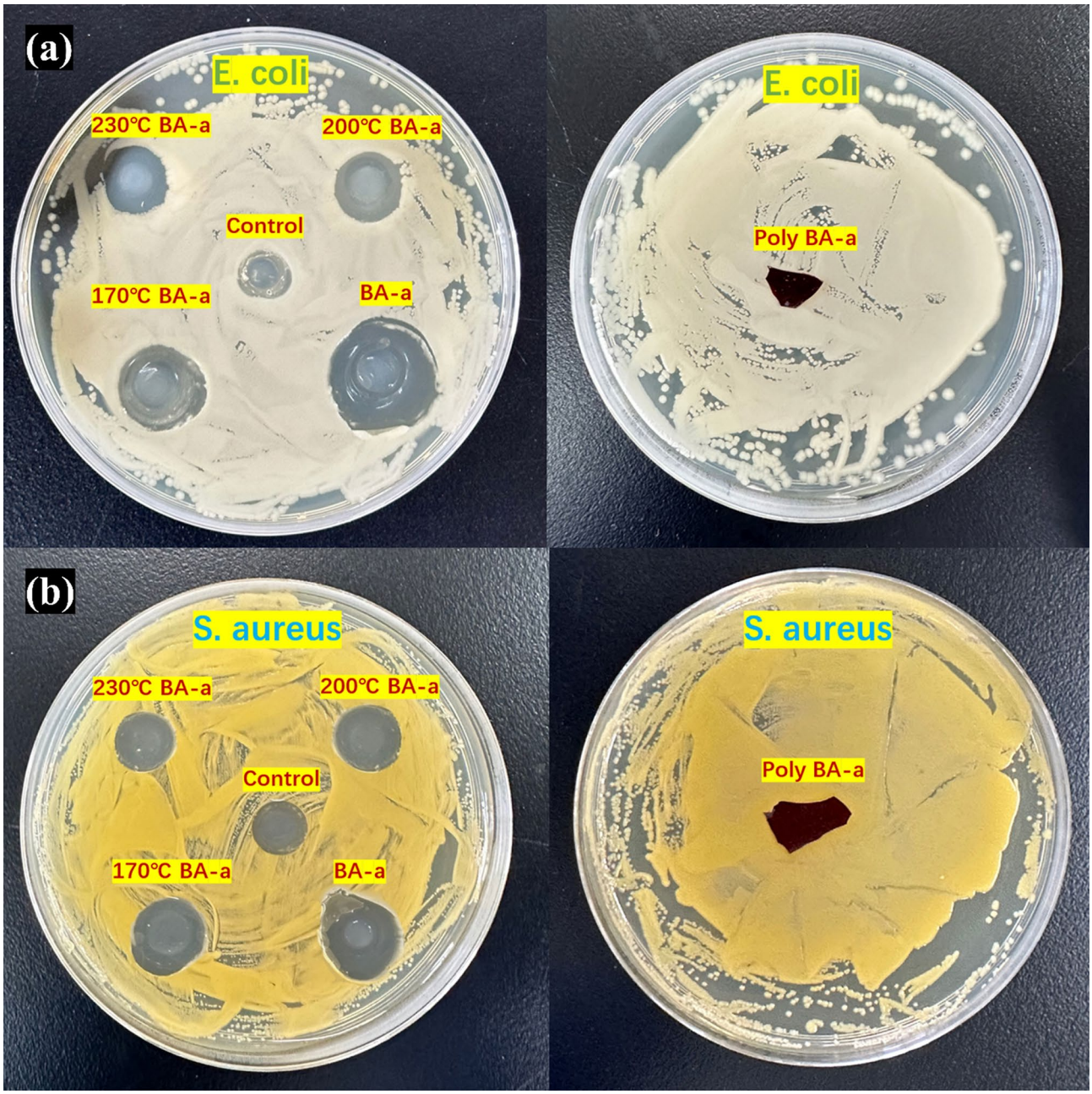

Fig. 3 Zone of inhibition for BA-a in bacterial petri dishes: **a** E. coli; **b** S. aureus

and BA-a is set at 170 °C to minimize the occurrence of the polymerization reaction of BA-a and maintain a higher antibacterial activity.

Biological activity of PP/BA-a

The antibacterial properties of PP/BA-a composites were evaluated by co-culture and plate coating counting. Figure 4 shows the coating photos of E. coli and S. aureus on the plate after co-cultivation with PP/BA-a, while Fig. 5 shows the statistical graph of antibacterial rate. From Fig. 4(a), it can be seen that PP lacks antibacterial performance, as there are still 256 colonies of E. coli present in the culture dish even when the washing solution is diluted 10^2 times. Similarly, as seen from Fig. 4(b), even after diluting the S. aureus washing solution 10^2 times, there are still 118 colonies on the agar plate. However, after adding BA-a, PP gained antibacterial properties. With the increase of BA-a content, the antibacterial performance also improved gradually. It can be seen that when the addition amount is 0.4 wt%, the PP/0.4BA-a

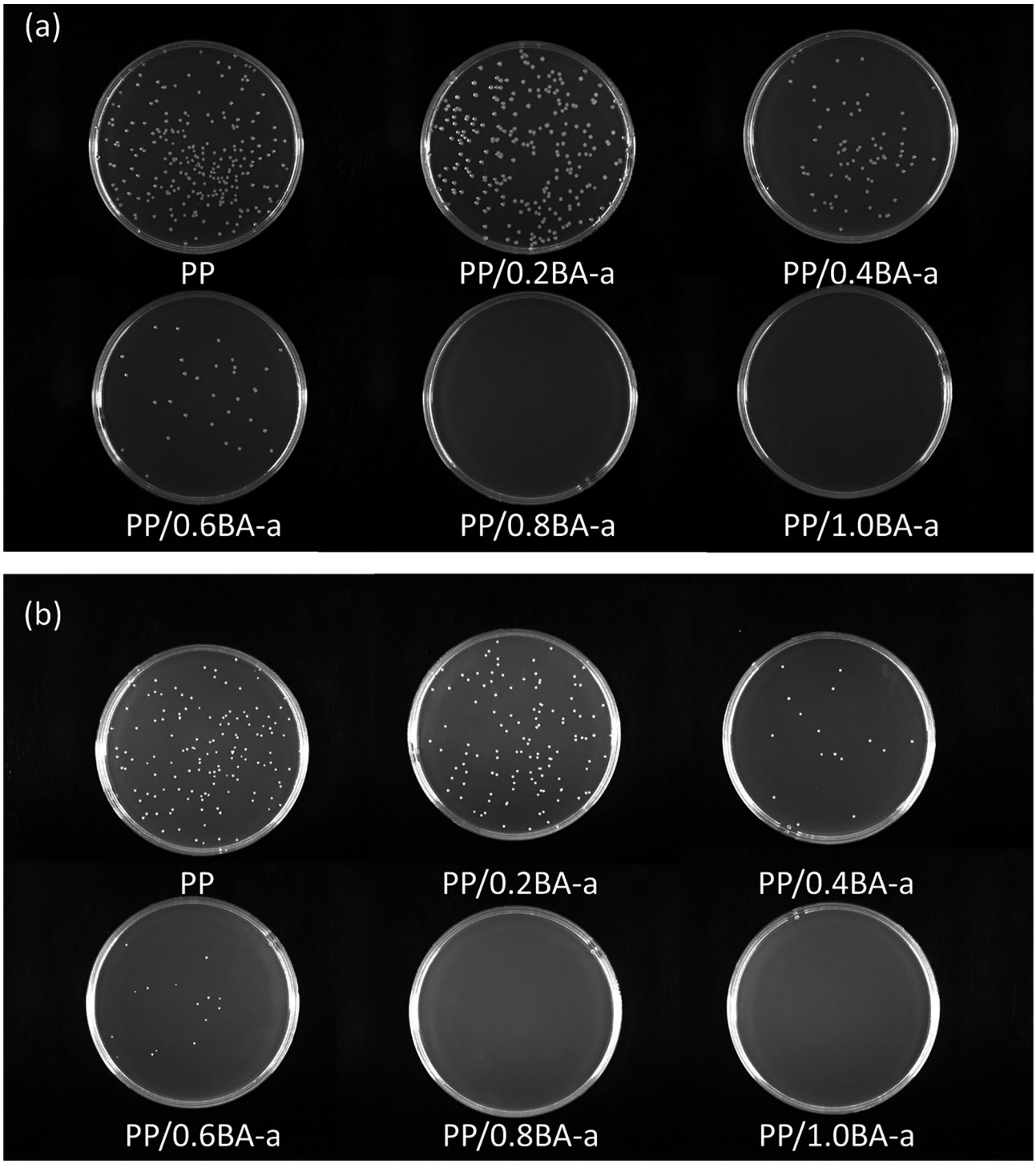

Fig. 4 Antibacterial activity: **a** E. coli; **b** S. aureus

composite material exhibits antibacterial performance, with an inhibition rate of 30.3% against E. coli and 19.7% against S. aureus. It can be seen that compared with S. aureus, PP/BA-a composite material has a better inhibition effect on E. coli. This may be related to the structure of the two kinds of bacteria. E. coli is a typical Gram negative bacterium, while S. aureus is a typical Gram positive bacterium. The dense skin polysaccharide layer on the outer layer of Gram positive bacteria can serve as a barrier protection, preventing the addition of antibacterial agents into cells and causing damage to the cytoplasm [36, 37]. Gram negative bacteria lack such a dense protective layer, which may be the reason

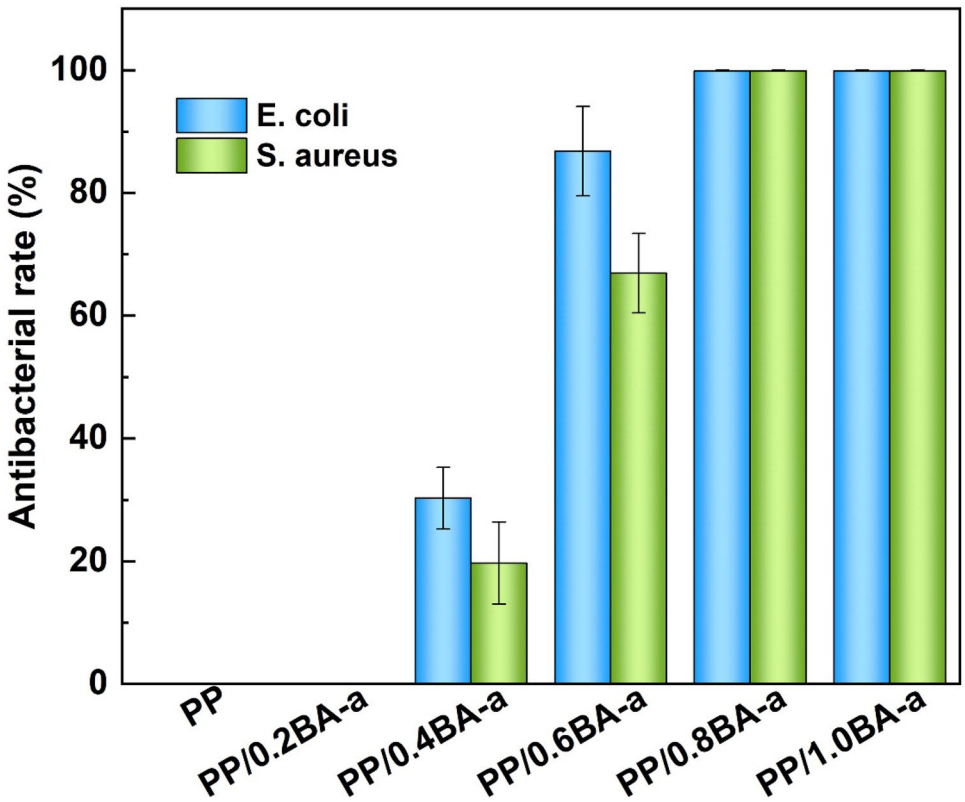

Fig. 5 Antibacterial activity of PP/BA-a

why BA-a has better antibacterial effects on E. coli. When the addition amount reached 0.8 wt%, the antibacterial effect of PP/0.8BA-a composites against E. coli and S. aureus could reach 99.9%, showing excellent antibacterial performance.

Moreover, through SEM images, it can be observed that a large number of E. coli adhere to the surface of untreated PP, as shown in Fig. 6(a), and they appear rod-shaped. Similarly, Fig. 7(a) reveals that a large number of S. aureus adhere to the surface of PP, and they appear spherical. However, after adding 0.4 wt% BA-a, it can be seen from Figs. 6(b) and 7(b) that the E. coli and S. aureus on the surface of PP/0.4BA-a start to rupture and deform, but some of their shapes still remain intact, which is consistent with the antibacterial results. Moreover, Figs. 6(c) and 7(c) show no adhesion of E. coli or S. aureus on the surface of PP/0.8BA-a, indicating that PP/0.8BA-a not only possesses good antibacterial performance but also inhibits bacterial adhesion.

In addition to antibacterial properties, antibacterial stability is also very important for materials. It has been proved

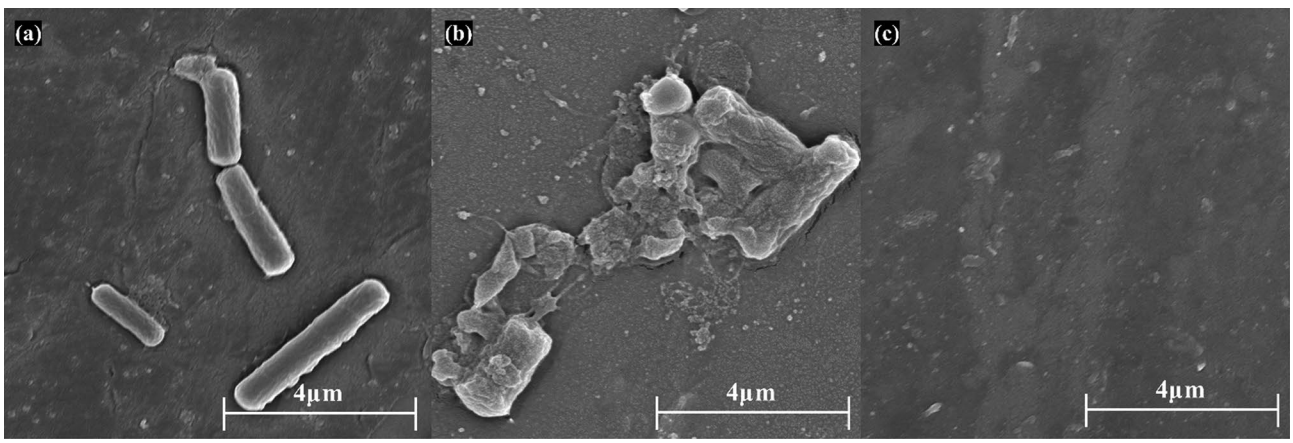

Fig. 6 SEM images of PP/BA-a against E.coli: **a** PP; **b** PP/0.4BA-a; **c** PP/0.8BA-a

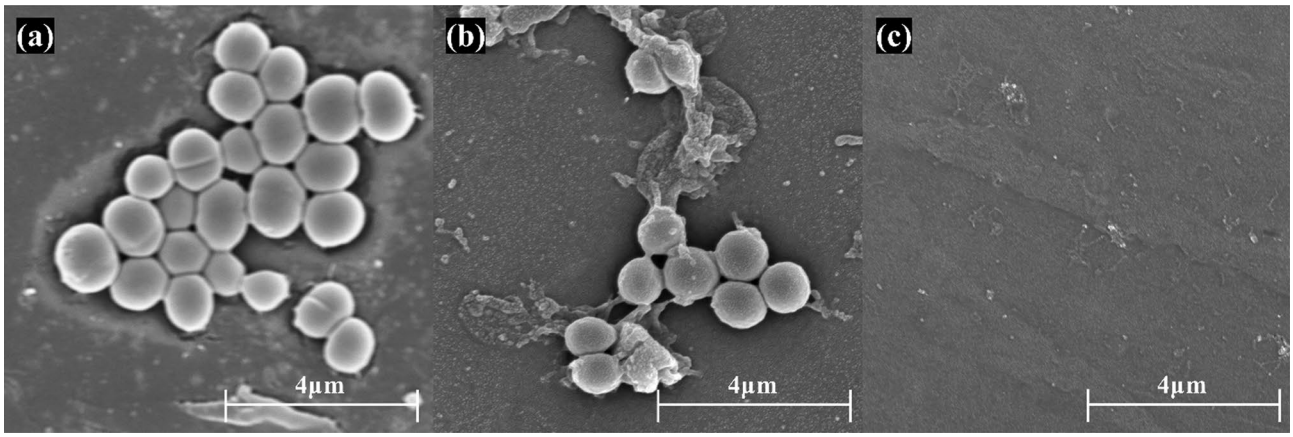

Fig. 7 SEM images of PP/BA-a against S. aureus: **a** PP; **b** PP/0.4BA-a; **c** PP/0.8BA-a

that PP/BA-a has excellent antibacterial properties, and the antibacterial stability will be further explored in the next step. The PP/ 0.8BA-a samples were soaked in ethyl acetate and ethanol for 7 days, and the leaching of BA-a on each day was detected by UV to characterize the migration of the antibacterial agent.

Figure 8 was chosen as the solvent because BA-a has a better solubility in ethyl acetate. It can be seen that the migration of BA-a in ethyl acetate reaches the highest on the seventh day and is still less than 1%, indicating a low migration. This is because of the good compatibility of BA-a and PP. The choice of ethanol as solvent is to simulate the disinfection scene in daily life; The choice of PBS as the solvent is to simulate the scenario of daily use. It can be seen that BA-a has little migration in ethanol and PBS. Among them, the migration in ethanol solvent is slightly higher than that in PBS solvent, which is because ethanol solvent is an organic solvent. The low migration also indicates that PP/0.8BA-a has strong antibacterial stability. In general, PP/0.8BA-a composites have good antibacterial properties and antibacterial stability, which indicates that the composites have a good application prospect.

In addition to antibacterial performance and antibacterial stability, the potential toxicity of organic antibacterial agents to the human body has always been a topic of great concern. Therefore, we conducted a cytotoxicity test.

According to the results of the MTT experiment, the relative activity of L929 cells co-cultured with 100% extract of PP/0.8BA-a for 1–5 days was above 98% (Fig. 9). According to the GB/T 16886.5–2017 standard, no significant decrease in cell proliferation was observed in the extract, indicating that the extract has a cell toxicity level of 1 and will not

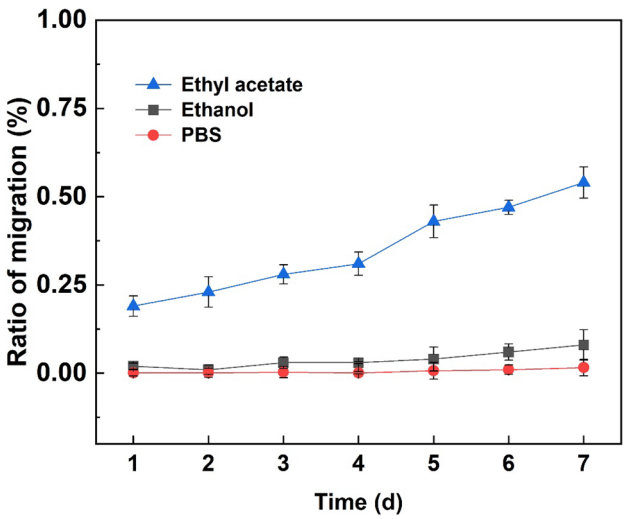

Fig. 8 Migration of BA-a in different solvent

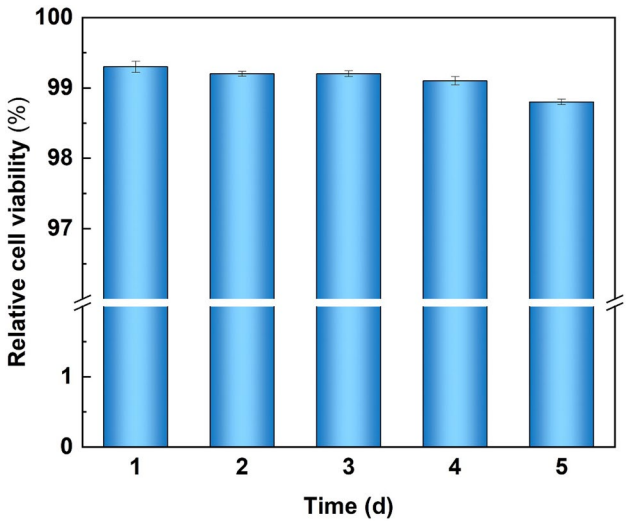

Fig. 9 Results of the cytotoxicity of L929 cells in vitro of PP/0.8BA-a

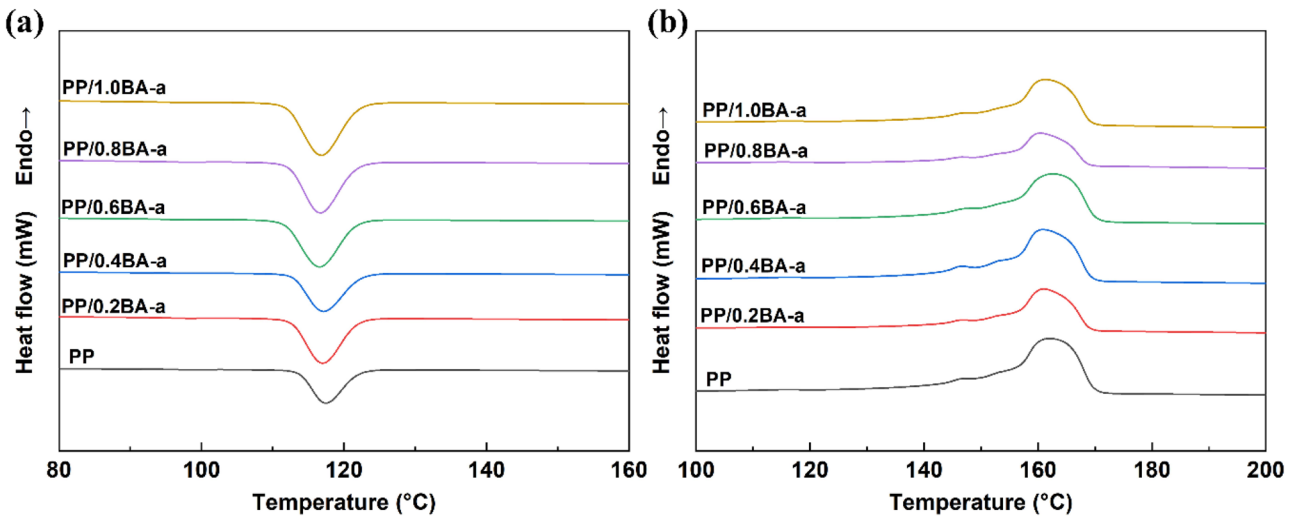

Fig. 10 The DSC curves of PP/BA-a: **a** DSC cooling curves; **b** DSC heating curves

cause harm to the human body. This result indicates that the PP/BA-a extract is non-toxic and can be used in medical materials.

Physical properties of PP/BA-a

Figure 10 and Table 3 is the crystallization data of PP/BA-a, in which the crystallinity is tested and calculated using the following Eq. (2)

$$X_c = \frac{\Delta H_m}{\Delta H_f} \times 100\% \quad (2)$$

ΔHf——PP enthalpy of complete melting, which is 209 J/g [38].

It can be seen that the addition of BA-a has no great influence on the crystallization behavior of PP. The melting temperature and crystallization temperature did not change much. However, the enthalpy of secondary melting and the crystallinity are increased. Moreover, the addition amount has little influence on the crystallinity, no matter the addition of 0.2 wt% or 1 wt%, the crystallinity is increased from 33% to around 36%, which is 3% higher than neat PP.

The glass transition temperature (T_g) refers to the temperature corresponding to the polymer material from the glass state to the high elastic state, which directly affects the service performance and process performance of the material. Figure 11 is the tangent curve of loss Angle with temperature, and the peak temperature of the curve is T_g. The addition of BA-a resulted in a slight increase in T_g, but in general, the change was not significant. The T_g of PP/BA-a composites are always maintained at about 6.5 °C.

Table 3 The relationship between curing degree and antibacterial activity

Sample	T_c/ °C	T_m/ °C	ΔH_m/ J•g^{-1}	X_c/ %
PP	117.81	160.40	69.87	33.43
PP/0.2BA-a	117.43	161.16	76.67	36.68
PP/0.4BA-a	117.53	160.84	76.52	36.61
PP/0.6BA-a	117.13	162.74	76.28	36.50
PP/0.8BA-a	117.16	160.78	77.01	36.85
PP/1.0BA-a	117.35	162.09	76.23	36.47

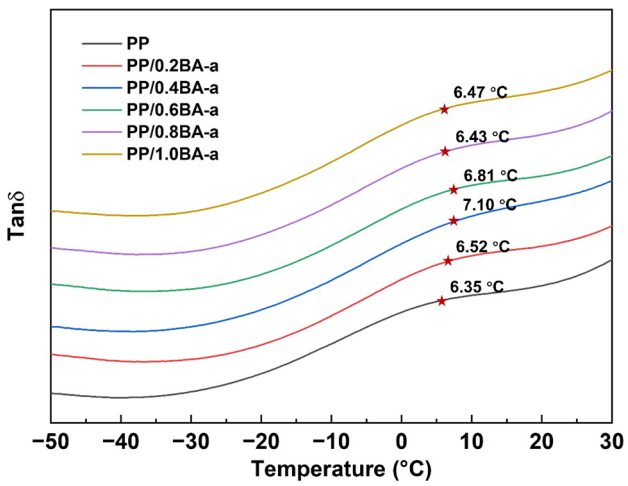

Fig. 11 The glass transition temperature of PP/BA-a

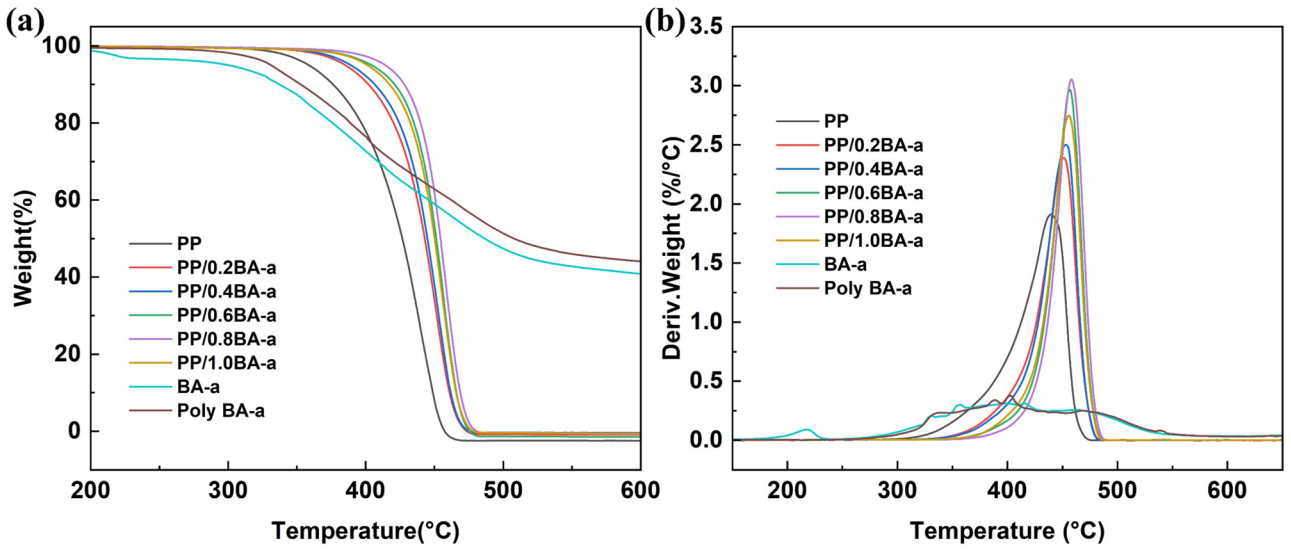

Fig. 12 **a** The TG curves of PP/BA-a and BA-a; **b** The DTG curves of PP/BA-a and BA-a

The PP/BA-a composites were analyzed by thermogravimetric analysis. The addition of BA-a has a certain effect on the thermal stability of PP. Figure 12 shows the TG curves and the DTG curves. The temperatures at 5% weight loss ($T_{5\%}$), 10% weight loss ($T_{10\%}$), 10% weight loss ($T_{10\%}$) and maximum weight loss (T_{max}) are shown in Table 4.

As a thermosetting resin, BA-a has good thermal stability. From Fig. 12(a), it can be seen that the TG curve of BA-a shows the first weight loss occurring at approximately 240 °C, consistent with the DSC results. This is because the monomer undergoes ROP process and releases CO_2 and some low molar mass compounds. When comparing BA-a and Poly BA-a with PP, it is found that both BA-a and Poly BA-a have lower weight than PP before 400 °C, but higher weight than PP after 400 °C, and there is still about 40% residue at 600 °C. However, as shown in Fig. 12(a), with the addition of BA-a, PP/BA-a shows improved thermal stability compared to pure PP. This is because BA-a partially opens the ring, converting the oxygen atoms on the imidazole ring into phenolic hydroxyl groups. The phenolic hydroxyl groups combine with the carbon chain free radicals in PP, inhibiting the auto-oxidation process of the polymer and improving its thermal stability [39, 40]. With the increase in the amount of BA-a addition, the initial decomposition temperature gradually rises. When the addition amount is 0.8 wt%, it reaches the highest point, and the initial decomposition temperature($T_{5\%}$) increases by 56 °C compared to PP, while the initial decomposition temperature of PP/1.0BA-a decreases slightly. This may be because when the BA-a addition amount is less than 0.8 wt%, the phenolic hydroxyl group dominates the improvement of PP thermal stability, while when the BA-a addition amount exceeds 0.8 wt%, the poor thermal stability of BA-a itself leads to a decrease in the initial decomposition temperature of PP/BA-a. The addition of 0.8 wt% BA-a is also the saturation point for antibacterial performance of the material. Therefore, PP/0.8BA-a exhibits its excellent antibacterial performance and better thermal stability. It is suitable for medical materials and can better withstand high-temperature sterilization scenarios such as dry heat and moist heat.

Table 4 Thermal properties of PP/BA-a

Sample	$T_{5\%}$/ °C	$T_{10\%}$/ °C	$T_{50\%}$/ °C	T_{max}/ °C
PP	358.60	376.29	426.67	439.69
PP/0.2BA-a	385.21	402.04	442.94	451.24
PP/0.4BA-a	389.21	406.60	444.90	453.25
PP/0.6BA-a	404.23	421.03	451.29	456.55
PP/0.8BA-a	414.24	428.04	454.45	458.04
PP/1.0BA-a	401.30	417.35	450.13	455.82
BA-a	299.92	337.31	486.57	396.45
Poly BA-a	331.18	352.75	508.00	403.48

Figure 13 shows the mechanical properties of PP/BA-a, including tensile strength, flexural modulus, impact strength and elongation at break. It can be seen that the addition of BA-a reduces the tensile strength of PP, but the decrease is very small. The flexural modulus has a small amplitude fluctuation, and there is no obvious upward or downward trend. Both impact strength and elongation at break fluctuate slightly, but the overall change is not significant. It can be seen that BA-a has little effect on the rigidity and toughness of PP. In summary, both PP/BA-a and PP possess excellent mechanical properties, making them suitable for various applications in medical materials.

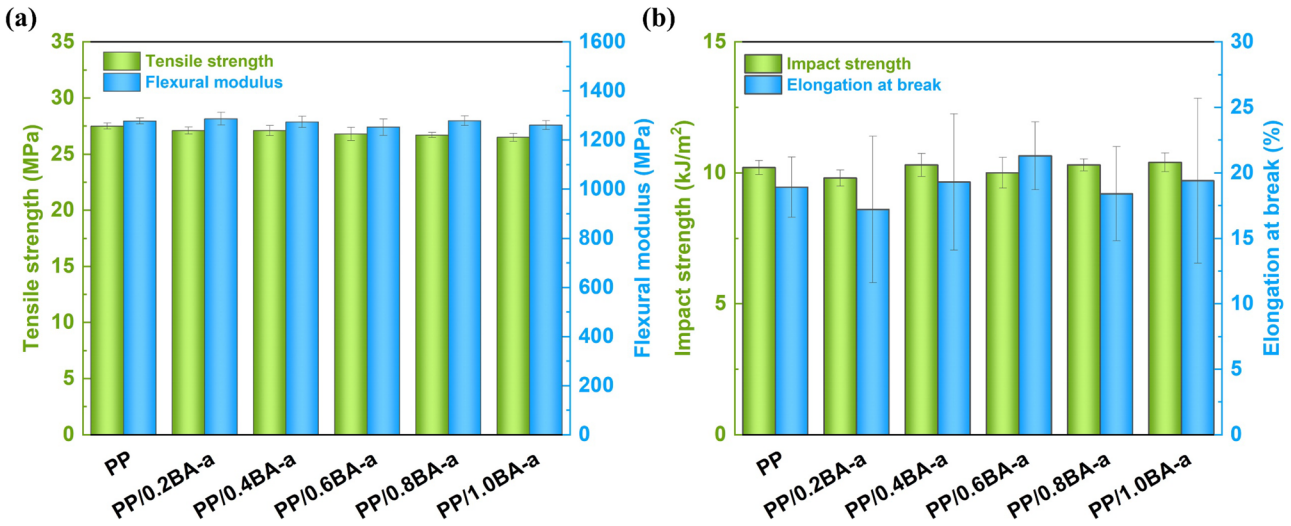

Fig. 13 The mechanical properties of PP/BA-a: **a** Tensile strength and Flexural strength; **b** Impact strength and Elongation at break

Conclusions

This study investigated the antibacterial modification of a common medical material PP. By blending bisphenol A benzoxazine (BA-a) with PP through melt blending, a new material, PP/BA-a, was obtained. It has been confirmed that BA-a exhibits good antibacterial activity, which is influenced by the degree of curing. Higher curing degree of BA-a leads to lower antibacterial activity. Therefore, a processing temperature of 170 °C was determined, and PP/0.8BA-a showed an antibacterial activity of 99.99% against both gram-negative and gram-positive bacteria. Additionally, migration tests revealed that PP/BA-a possesses good antibacterial stability. MTT experiments confirmed the non-toxicity of PP/BA-a extracts to L929 cells. Furthermore, TGA experiments verified the improved thermal stability of PP/BA-a, with an initial decomposition temperature increase of 56 °C compared to PP. The benzoxazine used in this paper is a common and widely studied benzoxazine, which effectively expands the application field of benzoxazine resin, and also provides a new idea for enhancing the antibacterial property of PP. At the same time, the thermal stability of PP/BA-a is improved, which provides a valuable method for medical grade antibacterial modified PP materials. The method exhibits promising potential for practical applications.

Acknowledgements This work was supported by the National Natural Science Foundation of China (22178108, 22278139), the Innovation Program of Shanghai Municipal Education Commission (2019-01-07-00-02-E00061) and Shanghai Municipal Science and Technology Commission (21520761100).

Author contributions Zhong Xin: conceptualization, supervision, resources, project administration, writing – reviewing, editing, and funding acquisition; Xiaoyu Shang: investigation, validation, formal analysis, data curation, visualization, writing-original draft, writing – reviewing and editing; Changlu Zhou: conceptualization, supervision, resources, project administration, writing – reviewing; Xian Zhang: conceptualization, methodology, software, writing – reviewing and editing.

Funding The Innovation Program of Shanghai Municipal Education Commission, 2019–01-07–00-02-E00061, Zhong Xin, Shanghai Municipal Science and Technology Commission, 21520761100, Zhong Xin, National Natural Science Foundation of China, 22178108, Zhong Xin, 22278139, Changlu Zhou.

Data availability The data that support the findings of this study are available from the corresponding author upon reasonable request.

Declarations

Competing interest The authors declare no competing financial interest.

References

1. Gai K, Ren X, Chen J, Zhou X, Wan Q, Wang Q, Li Y (2023) Construction of Helically Oriented Syndiotactic Polypropylene/Isotactic Polypropylene Composites for Medical Interventional Tubes via Rotation Extrusion. Ind Eng Chem Res 62(2):971–981. https://doi.org/10.1021/acs.iecr.2c03446
2. Jain S, Goossens H, Duin MV, Lemstra P (2005) Effect of in situ prepared silica nano-particles on non-isothermal crystallization of polypropylene. Polymer 46:8805–8818. https://doi.org/10.1016/j.polymer.2004.12.062
3. Singha P, Locklin J, Handa H (2017) A review of the recent advances in antimicrobial coatings for urinary catheters. Acta Biomater 50:20–40. https://doi.org/10.1016/j.actbio.2016.11.070
4. Otter JA, Donskey C, Yezli S, Douthwaite S, Goldenberg SD, Weber DJ (2016) Transmission of SARS and MERS coronaviruses and influenza virus in healthcare settings: the possible role

of dry surface contamination. J Hosp Infect 92:235–250. https://doi.org/10.1016/j.jhin.2015.08.027
5. Moore M (2020) The ICEL Healthcare-Associated Infection Probability Equation. Infect Control Hosp Epidemiol 41:s405–s406. https://doi.org/10.1017/ice.2020.1056
6. Kramer A, Schwebke I, Kampf G (2006) How long do nosocomial pathogens persist on inanimate surfaces? A systematic review BMC Infect Dis 6:130. https://doi.org/10.1186/1471-2334-6-130
7. Skvortsova A, Kocianova A, Guselnikova O, Elashnikov R, Burtsev V, Rimpelova S, Svobodova PV, Fitl P, Lukesova M, Kolska Z, Švorčík V, Lyutakov O (2023) Self-activated antibacterial MOF-based coating on medically relevant polypropylene. Appl Surf Sci 623:157048. https://doi.org/10.1016/j.apsusc.2023.157048
8. Tsou CH, Yao WH, Hung WS, Suen MC, De GM, Chen J, Tsou CY, Wang RY, Chen JC, Wu CS (2018) Innovative Plasma Process of Grafting Methyl Diallyl Ammonium Salt onto Polypropylene to Impart Antibacterial and Hydrophilic Surface Properties. Ind Eng Chem Res 57:2537–2545. https://doi.org/10.1021/acs.iecr.7b04693
9. Mitra D, Li M, Wang R, Tang Z, Kang ET, Neoh KG (2016) Scalable Aqueous-Based Process for Coating Polymer and Metal Substrates with Stable Quaternized Chitosan Antibacterial Coatings. Ind Eng Chem Res 55:9603–9613. https://doi.org/10.1021/acs.iecr.6b02201
10. Dai C, Lin J, Li H, Shen Z, Wang Y, Velkov T, Shen J (2022) The Natural Product Curcumin as an Antibacterial Agent: Current Achievements and Problems. Antixidants 11:459. https://doi.org/10.3390/antiox11030459
11. Poonam T, Madhuri S, Himani K, Anita K, Kasturi M, Dongsheng ZJPO (2015) Bactericidal Activity of Curcumin I Is Associated with Damaging of Bacterial Membrane. PLoS ONE 10(3):e0121313. https://doi.org/10.1371/journal.pone.0121313
12. Zheng X, Li Y, Li W, Pei X, Ye D (2023) Chitosan derived efficient and stable Pd nano-catalyst for high efficiency hydrogenation. Int J Biol Macromol 241:124615. https://doi.org/10.1016/j.ijbiomac.2023.124615
13. Odalanowska M, Woźniak M, Ratajczak I, Zielińska D, Cofta G, Borysiak S (2021) Propolis and Organosilanes as Innovative Hybrid Modifiers in Wood-Based Polymer Composites. Materials (Basel) 14:464. https://doi.org/10.3390/ma14020464
14. Breloy L, Ouarabi CA, Brosseau A, Dubot P, Brezova V, Abbad AS, Malval JP, Versace DL (2019) β-Carotene/Limonene Derivatives/Eugenol: Green Synthesis of Antibacterial Coatings under Visible-Light Exposure. ACS Sustain 7(24):19591–19604. https://doi.org/10.1021/acssuschemeng.9b04686
15. Huang T, Qian Y, Wei J, Zhou C (2019) Polymeric Antimicrobial Food Packaging and Its Applications. Ploymers 11:560. https://doi.org/10.3390/polym11030560
16. Chaloupka K, Malam Y, Seifalian AM (2010) Nanosilver as a new generation of nanoproduct in biomedical applications. Trends Biotechnol 28:580–588. https://doi.org/10.1016/j.tibtech.2010.07.006
17. Lansdown ABG (2010) A pharmacological and toxicological profile of silver as an antimicrobial agent in medical devices. Adv Pharmacol Sci 2010:910686. https://doi.org/10.1155/2010/910686
18. Danilczuk M, Lund A, Sadlo J, Yamada H, Michalik J (2006) Conduction electron spin resonance of small silver particles. Spectrochim Acta A Mol Biomol Spectrosc 63:189–191. https://doi.org/10.1016/j.saa.2005.05.002
19. Batitute V, Diler IS, Sozen B, Saltik CS, Akyildiz HI (2024) J Polym Res 31:28. https://doi.org/10.1007/s10965-024-03881-0
20. Wang Y, Liu LZ, Tian C, Wang Y, Song L, Shi Y (2023) Crystallization, morphology, optical properties, tear properties and antibacterial properties of nano zinc oxide composites. J Polym Res 30:352. https://doi.org/10.1007/s10965-023-03720-8
21. Rawat J, Kumar V, Ahlawat P, Tripathi LK, Tomar R, Kumar R, Dholpuria S, Gupta PK (2023) Current Trends on the Effects of Metal-Based Nanoparticles on Microbial Ecology. Appl Biochem Biotechnol 195:6168–6182. https://doi.org/10.1007/s12010-023-04386-0
22. Urbaniak M, Baran A, Giebułtowicz J, Bednarek A, Serwecińska L (2024) The occurrence of heavy metals and antimicrobials in sewage sludge and their predicted risk to soil — Is there anything to fear? Sci Total Environ 912:168856. https://doi.org/10.1016/j.scitotenv.2023.168856
23. Sánchez LE, Gomes D, Esteruelas G, Bonilla L, Lopez MAL, Galindo R, Cano A, Espina M, Ettcheto M, Camins A, Silva AM, Durazzo A, Santini A, Garcia ML, Souto EB (2020) Metal-Based Nanoparticles as Antimicrobial Agents: An Overview. Nanomaterials 10:292. https://doi.org/10.3390/nano10020292
24. Urbano VR, Peres MS, Maniero MG, Guimarães JR (2017) Abatement and toxicity reduction of antimicrobials by UV/H2O2 process. J Environ Manag 193:439–447. https://doi.org/10.1016/j.jenvman.2017.02.028
25. Gao Y, Wang J, Liu X, Lang X, Niu H (2023) Fabrication of durable and non-leaching triclosan-based antibacterial polypropylene. Eur Polym J 187:111892. https://doi.org/10.1016/j.eurpolymj.2023.111892
26. Ruszkiewicz JA, Li S, Rodriguez MB, Aschner M (2017) Is Triclosan a neurotoxic agent? J Toxicol Environ Health Part B 20:104–117. https://doi.org/10.1080/10937404.2017.1281181
27. Tabari SA, Esfahani ML, Hosseini SM, Rahimi A (2019) Neurobehavioral toxicity of triclosan in mice. Food Chem Toxicol 130:154–160. https://doi.org/10.1016/j.fct.2019.05.025
28. Bo C, Sha Y, Song F, Zhang M, Hu L, Jia P, Zhou Y (2022) Renewable benzoxazine-based thermosets from cashew nut: Investigating the self-healing, shape memory, recyclability and antibacterial activity. J Cleaner Prod 341:130898. https://doi.org/10.1016/j.jclepro.2022.130898
29. Zafar F, Khan S, Ghosal A, Azam M, Sharmin E, Rizwanul HQM, Nishat N (2019) Clean synthesis and characterization of green nanostructured polymeric thin films from endogenous Mg (II) ions coordinated methylolated-Cashew nutshell liquid. J Cleaner Prod 238:117716. https://doi.org/10.1016/j.jclepro.2019.117716
30. Mohamed MG, Li CJ, Khan MAR, Liaw CC, Zhang K, Kuo SW (2022) Formaldehyde-Free Synthesis of Fully Bio-Based Multifunctional Bisbenzoxazine Resins from Natural Renewable Starting Materials. Macromolecules 55:3106–3115. https://doi.org/10.1021/acs.macromol.2c00417
31. Tang Z, Chen W, Zhu Z, Liu H (2011) Synthesis of 2,3-diaryl-3,4-dihydro-2H-1,3-benzoxazines and their fungicidal activities. J Heterocycl Chem 48(33):255–260. https://doi.org/10.1002/jhet.533
32. Zahorulko SP, Varenichenko SA, Farat OK, Markova IV, Markov VI (2019) Investigation of Antimicrobial Activity of 1,3-benzoxazine Derivatives. Biopolym Cell 35:349–355. https://doi.org/10.7124/bc.000A12
33. Xin Z, Huang S (2023) The preparation and application of a supramolecular antibacterial material constructed by oxazine functional group. China Patent: CN 202311172821(9):2023
34. Zeng K, Huang J, Ren J, Ran QJMC (2018) Curing Reaction of Benzoxazine Under High Pressure and the Effect on Thermal Resistance of Polybenzoxazine. Macromol Chem Phys. https://doi.org/10.1002/macp.201800340
35. Bai Y, Yang P, Song Y, Zhu R, Gu Y (2016) Effect of hydrogen bonds on the polymerization of benzoxazines: influence and control. RSC Adv 6:45630–45635. https://doi.org/10.1039/c6ra08881c
36. Pismennõi D, Kattel A, Belouah I, Nahku R, Vilu R, Kobrin EG (2023) The Quantitative Measurement of Peptidoglycan Components Obtained from Acidic Hydrolysis in Gram-Positive and

Gram-Negative Bacteria via Hydrophilic Interaction Liquid Chromatography Coupled with Mass Spectrometry. Microorganisms 11(9):2134. https://doi.org/10.3390/microorganisms11092134
37. Mei L, Lu Z, Zhang W, Wu Z, Zhang X, Wang Y, Luo Y, Li C, Jia Y (2013) Bioconjugated nanoparticles for attachment and penetration into pathogenic bacteria. Biomaterials 34(38):10328–10337. https://doi.org/10.1016/j.biomaterials.2013.09.045
38. Li J, Cheung W, Jia DJP (1999) A study on the heat of fusion of β-polypropylene. Polymer 40(5):1219–1222. https://doi.org/10.1016/S0032-3861(98)00345-0
39. Arráez FJ, Arnal ML, Müller AJ (2018) Thermal and UV degradation of polypropylene with pro-oxidant. Abiotic characterization J Appl Polym Sci 135(14):46088. https://doi.org/10.1002/app.46088
40. Hoff A, Jacobsson S (2010) Thermal oxidation of polypropylene in the temperature range of 120–280 °C. J Appl Polym Sci 29(2):465–480. https://doi.org/10.1002/app.1984.070290203